Kinetics of ATP Hydrolysis during the DNA Helicase II-Promoted Unwinding of Duplex DNA†

Jaya G. Yodh and Floyd R. Bryant*

Department of Biochemistry, School of Hygiene and Public Health, The Johns Hopkins University, Baltimore, Maryland 21205

Received March 9, 1993

ABSTRACT: The ATP hydrolysis activity of DNA helicase II from *Escherichia coli* was examined in the presence of linear single-stranded DNA (ssDNA) and linear double-stranded DNA (dsDNA). In the presence of ssDNA, the ATP hydrolysis reaction followed a linear time course until the ATP was depleted. In the presence of dsDNA, in contrast, there was a kinetic lag before a linear phase of ATP hydrolysis was achieved. The nonlinear kinetics of the dsDNA-dependent ATP hydrolysis reaction could be modeled by a kinetic scheme in which helicase II undergoes a time-dependent transition from an ATPase-inactive to an ATPase-active form. Order of addition experiments indicated that this transition was not due to a rate-limiting association event between helicase II and any other component of the reaction. Instead, agarose gel assays showed that progressive unwinding of the dsDNA occurs during the same time period as the lag phase of the ATP hydrolysis reaction. No significant ATP hydrolysis was observed when the linear dsDNA was replaced with closed circular dsDNA, suggesting that the ATP hydrolysis reaction requires a dsDNA substrate that can be unwound to the complementary single strands. These results are consistent with a model in which the lag phase of the dsDNA-dependent ATP hydrolysis reaction corresponds to progressive unwinding of the dsDNA, with the ATP hydrolysis reaction arising from helicase II molecules that are bound to the separated single strands.

DNA helicase II (M_r 82 116), the product of the uvrD gene (Taucher-Scholz & Hoffmann-Berling, 1983; Hickson et al., 1983; Kumura & Sekiguchi, 1984), is a single-stranded DNA (ssDNA)[1]-dependent ATPase and promotes the ATP-dependent unwinding of duplex DNA. Helicase II has been implicated on the basis of genetic studies in DNA replication, repair, and recombination in *Escherichia coli* (Matson & Kaiser-Rogers, 1990). In addition, helicase II is required in reconstituted nucleotide excision repair (Caron et al., 1985; Husain et al., 1985) and methyl-directed mismatch repair (Lahue et al., 1989) systems.

It has been reported that the unwinding of duplex DNA by helicase II requires stoichiometric levels of protein, with each monomer able to unwind approximately 5 base pairs of DNA. This finding has been interpreted in terms of a mechanism in which a limited number of helicase II molecules first bind to the ends of a duplex DNA molecule to initiate the unwinding reaction. The bound helicase II molecules then direct a polar adsorption of additional helicase II molecules which continues as the complementary strands are separated (Kuhn et al., 1979). This mechanism is consistent with a recent electron microscopy study in which helicase II was shown to initiate unwinding at the ends of dsDNA molecules, and to remain bound to the separated strands of partially unwound dsDNA molecules (Runyon et al., 1990).

Although the helicase II-promoted DNA unwinding reaction is dependent on ATP hydrolysis, the kinetics of the ATP hydrolysis reaction and its relationship to DNA unwinding have not been characterized. In this paper, we examine the helicase II-catalyzed ATP hydrolysis reactions that occur in the presence of linear denatured DNA (ssDNA) and linear duplex DNA (dsDNA).

EXPERIMENTAL PROCEDURES

Materials

DNA helicase II was purified from *E. coli* strain N4830/pTL51 as described by Runyon et al. (1993). Circular ϕX dsDNA was prepared as described (Cox & Lehman, 1981), circular pUC18 and nicked circular pUC18 dsDNA were from Bethesda Research Laboratories (BRL), and nicked circular ϕX dsDNA was from New England Biolabs. ATP was from Pharmacia, [^{3}H]ATP was from ICN, and [γ-^{32}P]ATP was from Amersham.

Linear ϕX dsDNA was prepared by *Xho*I (BRL) cleavage of circular ϕX dsDNA; linear pUC18 dsDNA was prepared by *Eco*RI (BRL) cleavage of circular pUC18. Linear dsDNAs were ^{32}P-labeled at the 5′-termini using T4 polynucleotide kinase (BRL) and [γ-^{32}P]ATP as described (Maniatis et al., 1982). Linear dsDNAs were denatured to the complementary single strands by heating at 100 °C for 5 min. DNA concentrations were calculated using an A_{260} of 1 as equivalent to 36 μg/mL ssDNA and 50 μg/mL dsDNA. All DNA concentrations are expressed as total nucleotides.

Methods

ATP Hydrolysis Assay. ATP hydrolysis was measured using a thin-layer chromatography method as previously described (Weinstock et al., 1979). The reaction solutions (30 μL) contained 25 mM Tris-HCl (pH 7.5), 5% glycerol, 1 mM dithiothreitol, 50 μg/mL bovine serum albumin, 4.5

† This work was supported by Grant GM 36516 from the National Institutes of Health (F.R.B.) and Predoctoral Training Grant ES07141 from the National Institute of Environmental Health Science (J.G.Y.). A preliminary account of this work has been previously reported (Yodh & Bryant, 1992).

* Author to whom correspondence should be addressed. Telephone: (410) 955-3895.

[1] Abbreviations: ssDNA, single-stranded DNA; dsDNA, double-stranded DNA; ϕX, bacteriophage ϕX174; Tris, tris(hydroxymethyl)-aminomethane; EDTA, ethylenediaminetetraacetic acid.

0006-2960/93/0432-7765$04.00/0

mM $MgCl_2$, 4 mM [^{3}H]ATP, 1 μM DNA, and the concentrations of helicase II indicated in the figure legends. Unless otherwise indicated, all reactions were initiated by addition of helicase II after preincubation of all other components for 8 min at 37 °C. All reactions were carried out at 37 °C.

Agarose Gel Assay for DNA Unwinding. The DNA unwinding reaction solutions were identical to those for the ATP hydrolysis reactions described above except that unlabeled ATP and ^{32}P-labeled dsDNA were used. The reactions (100 μL) were initiated by the addition of helicase II after preincubation of all other reaction components for 8 min at 37 °C; the reactions were carried out at 37 °C. Aliquots (6.5 μL) of the reaction solutions were quenched at various times by the addition of 1% sodium dodecyl sulfate/22.5 mM EDTA (final concentrations). Gel loading dye was added (0.15% Bromophenol Blue/5% glycerol final concentrations), and the samples were loaded onto a 0.8% agarose gel and electrophoresed in TAE buffer (40 mM Tris–acetate/1 mM EDTA) for 11 h at 35 V. An autoradiograph of the gel was prepared by drying the gel onto Whatman DE81 paper and exposing it to Kodak XAR-5 films with an intensifer screen for 11 h at −70 °C. For each time point, the bands corresponding to intact duplex DNA and to full-length single-stranded DNA were excised from the appropriate gel lane. The radioactivity of each gel slice was determined by liquid scintillation counting and normalized to the total radioactivity present in that lane. The amount of dsDNA present at each time point was expressed relative to the amount present at zero time; the amount of ssDNA at each time point was expressed relative to the amount of ssDNA that was generated by alkali denaturation (100 mM NaOH, 5 min at 25 °C) of the amount of dsDNA present at zero time. Time courses of DNA unwinding were constructed both from the decrease in the intact duplex DNA band and from the increase in the full-length single-stranded DNA band. No renaturation of ^{32}P-labeled linear denatured DNA was observed in either the presence or the absence of helicase II under these assay conditions.

RESULTS

Experimental Model. Although it has been shown that helicase II binds to ssDNA and catalyzes the ssDNA-dependent hydrolysis of ATP (Abdel-Monem et al., 1977a), the kinetics of ATP hydrolysis during the helicase II-promoted unwinding of duplex DNA have not been examined. We reasoned that when helicase II is first added to a limiting amount of duplex DNA (dsDNA), little if any helicase II would be bound to the DNA, and the observed rate of ATP hydrolysis would therefore be near zero. As the DNA unwinding reaction proceeds, however, helicase II molecules would become associated with the single-stranded DNA being generated and would thereby be activated for ATP hydrolysis. We therefore predicted that there would be an initial lag in the kinetics of the dsDNA-dependent ATP hydrolysis reaction which would reflect the progressive unwinding of the duplex DNA and that the maximal rate of ATP hydrolysis would be reached when all of the duplex DNA molecules had been completely unwound to the complementary single strands (Figure 1). In the presence of denatured DNA (ssDNA), in contrast, since the single strands are already separated, we expected that the helicase II molecules would bind directly to the DNA and that ATP hydrolysis would follow a linear time course.

The kinetics of dsDNA-dependent ATP hydrolysis that are predicted by the model in Figure 1 can be described by a scheme in which helicase II undergoes a time-dependent transition from a state with no ATPase activity, E (free helicase II), to a state that hydrolyzes ATP at the steady-state rate, v_{ss}, E* (DNA-bound helicase II) (Scheme I).

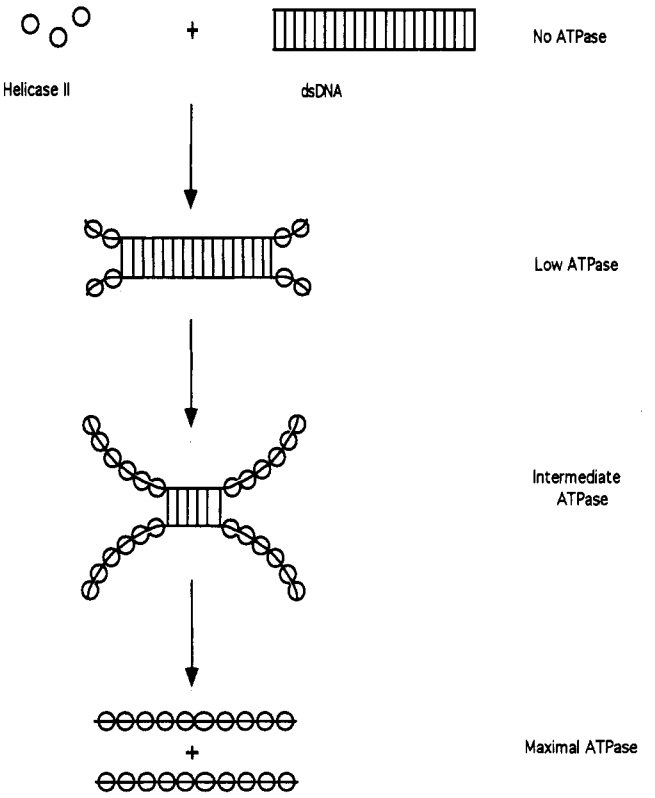

FIGURE 1: General model for the kinetics of ATP hydrolysis during the DNA helicase II-promoted unwinding of duplex DNA. See text for details. This model is intended only to illustrate a general relationship between the extent of DNA unwinding and the rate of ATP hydrolysis, and is not intended to represent the state of oligomerization of helicase II (Runyon et al., 1993) or the precise structures of the various helicase II–DNA reaction intermediates.

Scheme I

$$E \xrightarrow{k} E^*$$

The instantaneous rate of ATP hydrolysis at a given time (t) predicted by Scheme I is given by eq 1, where [ADP]

$$\frac{d[ADP]}{dt} = v_{ss} - v_{ss}e^{-kt} \quad (1)$$

represents the concentration of the ATP hydrolysis product, ADP, and k is the apparent first-order rate constant for the transition between E and E* (the rate-determining step for the DNA unwinding reaction). Integration of eq 1 yields an expression for the concentration of product ADP at time t (eq 2). The ssDNA-dependent ATP hydrolysis time courses that

$$[ADP]_t = v_{ss}(t - k^{-1} + k^{-1}e^{-kt}) \quad (2)$$

are predicted by the model in Figure 1 can also be described by Scheme I. In this case, the lag times (k^{-1}) are equal to zero, and eq 2 reduces to eq 3:

$$[ADP]_t = v_{ss}t \quad (3)$$

ATP Hydrolysis by Helicase II in the Presence of Single- and Double-Stranded DNA. In order to test the model described in Figure 1, time courses of ATP hydrolysis at 4

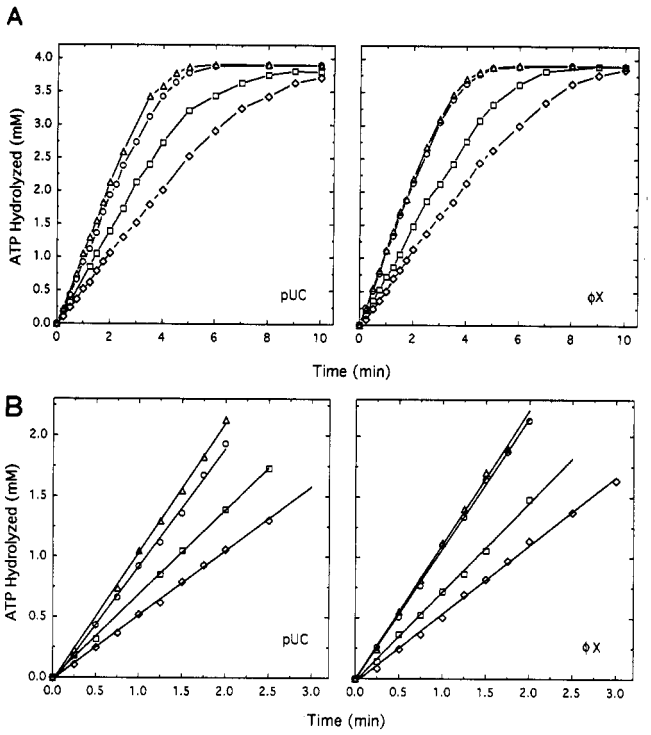

FIGURE 2: ATP hydrolysis by DNA helicase II in the presence of ssDNA. (Panel A) Reaction solutions contained 1 μM pUC18 ssDNA (*left*) or 1 μM ϕX ssDNA (*right*), 25 mM Tris-HCl (pH 7.5), 4.5 mM $MgCl_2$, 4 mM ATP, and 50 (◇), 100 (□), 200 (○), and 300 nM (△) helicase II. The reactions were carried out at 37 °C. The points represent the amount of ATP hydrolyzed as a function of time. (Panel B) The data from (A) have been expanded in order to more clearly display the initial phase of ATP hydrolysis. The simulated curves (solid lines) showing the amount of ATP hydrolyzed as a function of time were calculated using eq 3 and the kinetic parameters given in Table I.

mM ATP (K_m for ATP = 70 μM)[2] were measured for various concentrations of helicase II (50–300 nM) in the presence of a fixed concentration (1 μM) of either linear denatured DNA or linear duplex DNA. Two types of DNA were utilized in these studies: pUC18 DNA (2686 base pairs) and ϕX DNA (5386 base pairs).[3] All reactions were carried out at pH 7.5 and 37 °C.

The ATP hydrolysis time courses that were obtained with linear denatured pUC18 and ϕX DNA and various concentrations of helicase II are shown in Figure 2A. Each ssDNA-dependent ATP hydrolysis reaction followed a linear time course that continued until all of the ATP was hydrolyzed; no significant product inhibition by ADP was apparent in these reactions. These linear ATP hydrolysis time courses could be modeled by Scheme I (eq 3): the simulated curves that were derived for each time course are shown in Figure 2B as solid lines through the experimental data points, and the corresponding values of v_{ss} are given in Table I. In these reactions, the rate of ATP hydrolysis increased with increasing helicase II concentration until a maximal rate of approximately 1.0 mM ADP min^{-1} was attained at 200 nM helicase II. Since any helicase II in excess of that which is bound by the ssDNA will exhibit little ATP hydrolysis activity (the DNA-independent ATP hydrolysis rate was 0.05 mM ADP min^{-1} at 200 nM helicase II; see Figure 4),[4] the rates obtained at saturating helicase II concentrations presumably correspond to ssDNA molecules that are complexed with the maximal amount of helicase II possible. The observed rates of ATP hydrolysis (mM ADP min^{-1}), rather than turnover numbers (min^{-1}), are reported in Table I since the exact number of DNA helicase II monomers that are bound to the ssDNA under saturating conditions is not known.[5]

Table I: Kinetic Parameters for Helicase II-Catalyzed ATP Hydrolysis[a]

			dsDNA	
DNA	helicase II concn (nM)	ssDNA v_{ss} (mM ADP min^{-1})	v_{ss} (mM ADP min^{-1})	k^{-1} (min)
pUC	50	0.52	0.30	1.13
	100	0.69	0.61	1.01
	200	1.06	0.94	1.77
	300	0.98	1.07	1.79
ϕX	50	0.52	0.26	2.15
	100	0.73	0.52	2.04
	200	0.97	0.77	2.31
	300	1.00	0.69	2.20

[a] These parameters were obtained by fitting the data shown in Figure 2 to eq 3 and the data in Figure 3 to eq 2, using Enzfitter Version 1.05 [Leatherbarrow, R. J. (1987); Biosoft, Cambridge, U.K.].

The ATP hydrolysis time courses that were obtained with linear duplex pUC18 and ϕX DNA and various concentrations of helicase II are shown in Figure 3A. In contrast to the linear time courses that were obtained with ssDNA, the dsDNA-dependent ATP hydrolysis reactions exhibited a lag phase of approximately 1.0–1.8 min (pUC18 DNA) or 2.0–2.3 min (ϕX DNA) before a linear phase of hydrolysis was reached. These nonlinear ATP hydrolysis time courses could be modeled by Scheme I (eq 2): the simulated curves that were derived for each time course are shown in Figure 3B as solid lines through the experimental data points, and the corresponding values of k^{-1} and v_{ss} for each reaction are given in Table I. As with the ssDNA-dependent reactions, the linear phase of ATP hydrolysis in the dsDNA-dependent reaction increased in rate with increasing helicase II concentration until a maximal rate was attained at approximately 200 nM helicase II. The maximal rates in the pUC18 and ϕX dsDNA-dependent ATP hydrolysis reactions were approximately 1.0 and 0.77 mM ADP min^{-1}, respectively.

Dependence of dsDNA-Dependent ATP Hydrolysis on the Order of Addition. Although the ATP hydrolysis kinetics presented in the previous section are consistent with the DNA unwinding model shown in Figure 1, it was conceivable that the lag phase of the dsDNA-dependent ATP hydrolysis reaction was due simply to a slow association between helicase and a component of the reaction mixture. In the time courses shown in Figure 3, the lag generally appears to be independent of helicase II concentration, indicating that it is not due to a bimolecular association of helicase II with the ends of the dsDNA molecules. To investigate the possibility that the lag was due to a slow association between helicase II and another component of the reaction mixture, a series of dsDNA-

[2] J. G. Yodh and F. R. Bryant, unpublished results.

[3] Although the linear DNA experiments reported in this paper were carried out with *Eco*RI-cut pUC18 DNA and *Xho*I-cut ϕX DNA (four unpaired bases at the 5′-termini), we have obtained similar results with *Pst*I-cut pUC18 (four unpaired bases at the 3′-termini) and *Sma*I-cut pUC18 and *Ssp*I-cut ϕX DNA (blunt-ended termini).

[4] DNA-independent ATP hydrolysis activity was also reported by Runyon et al. (1993).

[5] We have estimated the ssDNA binding site size for helicase II to be approximately 10 nucleotides; this estimate is based on the minimal oligomer size required for full activation of the ssDNA-dependent ATP hydrolysis activity (J. G. Yodh and F. R. Bryant, preliminary results). Lohman and co-workers have estimated a minimum site size of 10 (±2) nucleotides per helicase monomer on the basis of fluorescence quenching measurements (Runyon et al., 1993).

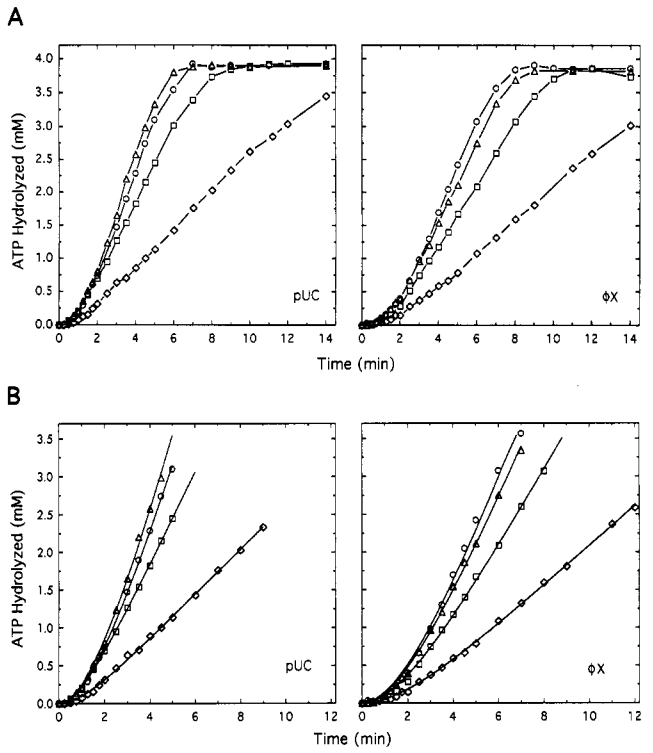

FIGURE 3: ATP hydrolysis by DNA helicase II in the presence of dsDNA. (Panel A) Reaction solutions contained 1 μM pUC18 dsDNA (*left*) or 1 μM ϕX dsDNA (*right*), 25 mM Tris-HCl (pH 7.5), 4.5 mM $MgCl_2$, 4 mM ATP, and 50 (◇), 100 (□), 200 (○), and 300 nM (△) helicase II. The reactions were carried out at 37 °C. The points represent the amount of ATP hydrolyzed as a function of time. (Panel B) The data from (A) have been expanded in order to more clearly display the initial phase of ATP hydrolysis. The simulated curves (solid lines) showing the amount of ATP hydrolyzed as a function of time were calculated using eq 2 and the kinetic parameters given in Table I.

dependent ATP hydrolysis reactions was carried out as described in Figure 3 (200 nM helicase II reactions), except that the order of addition of the reaction components was varied. In each reaction, all components, except for helicase II and the initiation component (either ATP, $MgCl_2$ plus ATP, DNA, $MgCl_2$ plus DNA, $MgCl_2$, or DNA plus ATP), were incubated at 37 °C for 6 min. Helicase II was then added, and the incubation was continued for an additional 2 min; this time period approximated the lag time observed at saturating helicase II concentrations (Table I) and thus should have been sufficient to allow any slow association events to occur. The ATP hydrolysis reaction was then initiated by addition of the final component of the reaction mixture.

As shown in Figure 4, a lag phase was observed for the pUC18 and ϕX dsDNA-dependent ATP hydrolysis reactions, regardless of the order of addition that was followed. These results indicate that the lag phase is not due to a slow association between helicase II and either ATP, MgATP, DNA, MgDNA, $MgCl_2$, or DNA and ATP. Also, the maximal rates of ATP hydrolysis were similar regardless of the order of addition.

Dependence of dsDNA-Dependent ATP Hydrolysis on DNA Structure. In order to investigate the effect of dsDNA structure on the kinetics of the dsDNA-dependent ATP hydrolysis reaction, time courses of ATP hydrolysis were measured in the presence of nicked circular pUC18 dsDNA and closed circular pUC18 dsDNA at saturating concentrations of helicase II (200 nM).

As shown in Figure 5, the time course of ATP hydrolysis in the presence of nicked circular pUC18 dsDNA was similar to that obtained with linear pUC18 dsDNA (Figure 3). Thus,

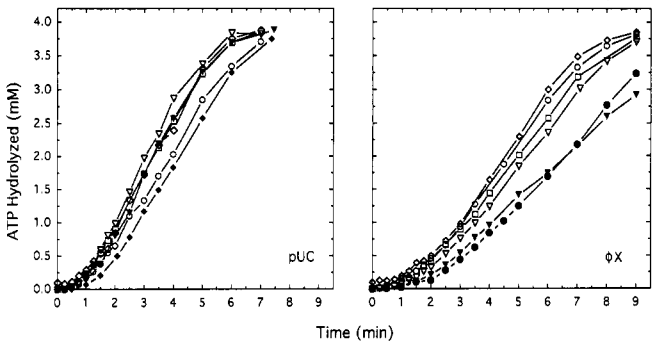

FIGURE 4: Dependence of dsDNA-dependent ATP hydrolysis on the order of addition. Reaction solutions contained 1 μM linear pUC18 dsDNA (*left*) or ϕX dsDNA (*right*), 25 mM Tris-HCl (pH 7.5), 4.5 mM $MgCl_2$, 4 mM ATP, and 200 nM helicase II. Reactions were initiated by the addition of DNA (◇), $MgCl_2$ plus DNA (○), ATP (▼), $MgCl_2$ plus ATP (▽), $MgCl_2$ (□), or DNA plus ATP (●). The reactions were carried out at 37 °C. The points represent the amount of ATP hydrolyzed as a function of time. Note that the DNA-initiated reactions contained 0.2 mM ADP at time zero; this was generated by the DNA-independent ATP hydrolysis activity of the helicase II preparation during the 2-min preincubation period.

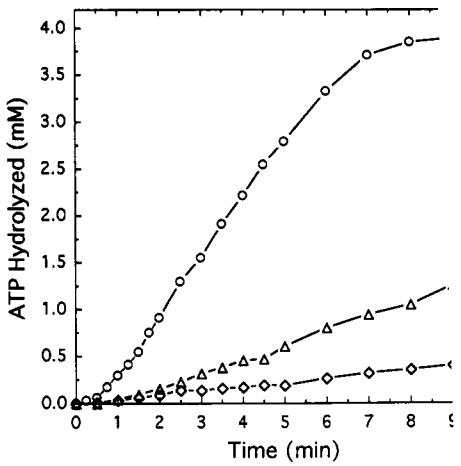

FIGURE 5: Dependence of dsDNA-dependent ATP hydrolysis on DNA structure. Reaction solutions contained 25 mM Tris-HCl (pH 7.5), 4.5 mM $MgCl_2$, 4 mM ATP, 200 nM helicase II, and 1 μM nicked circular pUC18 dsDNA (○), 1 μM covalently closed pUC18 dsDNA (△), or no DNA (◇). The reactions were carried out at 37 °C. The points represent the amount of ATP hydrolyzed as a function of time.

the different structures of these two DNA molecules have little effect on the molecular event(s) responsible for the lag in the dsDNA-dependent ATP hydrolysis reaction. Although ATP hydrolysis was also observed in the presence of closed circular pUC18 dsDNA, the rate (0.15 mM ADP min^{-1}) was only 20% of that obtained with the corresponding linear dsDNA (Table I); this ATPase activity was likely due to contamination of the closed circular dsDNA with nicked circular and linear dsDNA, which was determined by agarose gel densitometry to be 25% (data not shown). Thus, little or no ATP hydrolysis activity could be attributed to the interaction of helicase II with closed circular dsDNA. Similar results were obtained using nicked circular and closed circular ϕX dsDNA (data not shown). These results indicate that the dsDNA-dependent ATP hydrolysis reaction of helicase II requires a dsDNA substrate with a free end, possibly to enable the dsDNA to be unwound to the separated complementary single strands.

Agarose Gel Assay for DNA Unwinding by Helicase II. In order to determine if unwinding of the dsDNA indeed occurs during the lag phase of the dsDNA-dependent ATP hydrolysis reactions, reaction mixtures containing 1 μM ^{32}P-labeled linear

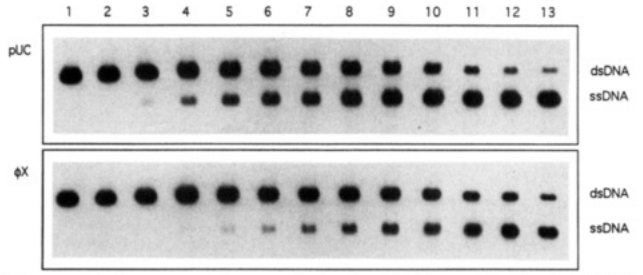

FIGURE 6: Agarose gel assay of duplex DNA unwinding by DNA helicase II. Reaction solutions contained 1 μM ^{32}P-labeled linear pUC18 dsDNA (*upper*) or 1 μM ^{32}P-labeled ϕX dsDNA (*lower*), 25 mM Tris-HCl (pH 7.5), 4.5 mM $MgCl_2$, 4 mM ATP, and 200 nM helicase II. Reactions were carried out at 37 °C, and analyzed by agarose gel electrophoresis followed by autoradiography. *Lanes 1–13* represent 0-, 0.25-, 0.5-, 0.75-, 1.0-, 1.25-, 1.5-, 2.0-, 2.5-, 3.0-, 4.0-, 5.0-, and 6.0-min reaction time points. The positions of the duplex DNAs (dsDNA) and the corresponding complementary single-stranded DNAs (ssDNA) are indicated.

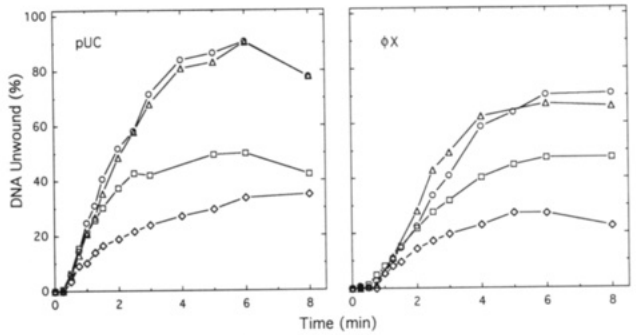

FIGURE 7: Dependence of duplex DNA unwinding on DNA helicase II concentration. Reaction solutions contained 1 μM ^{32}P-labeled linear pUC18 dsDNA (*left*) or 1 μM ^{32}P-labeled ϕX dsDNA (*right*), 25 mM Tris-HCl (pH 7.5), 4.5 mM $MgCl_2$, 4 mM ATP, and 50 (◇), 100 (□), 200 (○), and 300 nM (△) helicase II. The reactions were carried out at 37 °C and analyzed as described under Experimental Procedures. The points represent the amount of DNA unwound as a function of time.

duplex pUC18 or ϕX DNA, 4 mM ATP, and various concentrations of helicase II were analyzed by agarose gel electrophoresis. In this assay, the linear duplex DNAs are well separated from the corresponding linear denatured DNAs, and thus the conversion of the dsDNA substrate to the separated complementary single strands can be monitored. Representative autoradiographs that were obtained for reactions containing 200 nM helicase II are shown in Figure 6. In these and all other reactions, the appearance of ssDNA and the disappearance of dsDNA followed similar kinetic time courses; the time courses that are presented in graphical form below were based on the time-dependent appearance of ssDNA.

The time courses of the dsDNA unwinding reactions that were obtained with pUC18 or ϕX dsDNA and various concentrations of helicase II are shown in Figure 7. These time courses demonstrate clearly that unwinding of pUC18 and ϕX dsDNA does occur during the same time period as the lag phase (0–2 min) of the dsDNA-dependent ATP hydrolysis reactions (Figure 3). The pUC18 dsDNA unwinding reactions displayed an apparent lag of approximately 0.25 min which was followed by a linear phase of unwinding; the ϕX dsDNA reactions exhibited an apparent lag of approximately 0.75 min before the linear phase of unwinding began. The rate and extent of the DNA unwinding reaction depend on the helicase II concentration, with the maximal rate and extent being attained at approximately 200 nM helicase II for both DNAs. This finding is consistent with the saturation behavior observed in the dsDNA-dependent ATP hydrolysis reactions (Figure 3) and again indicates that this concentration of helicase II is sufficient to saturate 1 μM dsDNA.

Table II: Correlation of Steady-State ATP Hydrolysis Rates with Extent of DNA Unwinding[a]

DNA	helicase II concn (nM)	v_{ss}(ds)/v_{ss}(ss)	final extent of DNA unwinding (%)
pUC	50	0.58	34
	100	0.88	50
	200	0.89	86
	300	1.09	86
ϕX	50	0.50	27
	100	0.71	47
	200	0.79	70
	300	0.69	67

[a] These parameters were derived from the experimental data in Table I and Figure 7.

The maximal extent of dsDNA unwinding measured by the agarose gel assay at saturating concentrations of helicase II was approximately 85% for pUC18 DNA and 70% for ϕX DNA. As shown in Table II, these final extents correlate closely with the ratio of the steady-state rates of dsDNA-dependent and ssDNA-dependent ATP hydrolysis that were measured for these DNAs at saturating helicase II concentrations. This correlation suggests that the ATP hydrolysis reaction that is observed in the presence of dsDNA arises from helicase II molecules that are bound to the unwound complementary singie strands, and that the linear phase of the dsDNA-dependent ATP hydrolysis reaction (where the rate of ATP hydrolysis is greatest) reflects the final extent of dsDNA unwinding. At subsaturating concentrations of helicase II, the measured extents of DNA unwinding were somewhat less than would be predicted from the corresponding steady-state rates of ATP hydrolysis. Under subsaturating conditions, there may be a significant amount of partially unwound dsDNA molecules which would be reflected fully by the observed rate of ATP hydrolysis. The agarose gel assay, however, may underestimate the total amount of DNA unwinding that has occurred under these conditions because partially or transiently unwound strands that rapidly reanneal when the reaction time points are quenched with SDS (which removes helicase II from the DNA) will not be detected.

DISCUSSION

The ATP hydrolysis activity of DNA helicase II from *Escherichia coli* was examined in the presence of linear single-stranded DNA (ssDNA) and linear double-stranded DNA (dsDNA). The ssDNA-dependent ATP hydrolysis reactions followed a linear time course, whereas the dsDNA-dependent reactions exhibited a kinetic lag phase before a linear phase of ATP hydrolysis was achieved. There are several possible molecular events which could account for the lag phase in the dsDNA-dependent ATP hydrolysis reaction. For example, the lag phase could represent a slow association event between helicase II and another component of the reaction mixture (Mg^{2+} or ATP) which may be required before ATP hydrolysis can take place. This possibility seems unlikely, however, since no lag was observed in the ssDNA-dependent ATP hydrolysis reaction. Furthermore, the lag phase could not be eliminated by any combination of preincubation steps designed to allow slow association events to occur. These experiments, however, do not rule out the possibility that the lag phase is due to a slow assembly of a complex containing helicase II, Mg^{2+}, and ATP at an initiation site on dsDNA.

The substrate specificity of the dsDNA-dependent ATP hydrolysis reaction suggests that this reaction is related to the DNA unwinding reaction. Although ATP hydrolysis was observed with either linear duplex DNA or nicked circular duplex DNA, little if any ATP hydrolysis occurred in the presence of closed circular duplex DNA. This indicates that the dsDNA-dependent ATP hydrolysis reaction does not occur simply upon binding of helicase II to dsDNA, but rather that the reaction requires that the dsDNA be unwound to the separated complementary single strands. The similar ATP hydrolysis reaction time courses that were obtained with linear duplex DNA and nicked circular duplex DNA are consistent with the ability of helicase II to initiate unwinding either at the ends or at nicks in duplex DNA (Runyon & Lohman, 1989; Runyon et al., 1990).

The agarose gel assays in Figure 7 show that substantial unwinding of linear duplex DNA does occur during the same time period as the lag phase of the dsDNA-dependent ATP hydrolysis reaction. At saturating concentrations of helicase II, 30% of ϕX DNA and 50% of pUC18 DNA are *completely* unwound within the first 2 min of the reaction. Furthermore, the maximal extents of DNA unwinding that were obtained at saturating concentrations of helicase II correlate directly with the ratio of the dsDNA-dependent and ssDNA-dependent ATP hydrolysis rates that were measured under the same conditions. These observations are consistent with the idea that the ATP hydrolysis reaction that is observed in the presence of duplex DNA is due to helicase II molecules that are bound to the unwound complementary single strands.

The agarose gel assay presumably measures only the complete unwinding of duplex DNA, since any partially or transiently unwound DNA molecules should rapidly reanneal when the reaction time points are quenched with SDS (which removes helicase II from the DNA). Thus, the fact that both the pUC18 and ϕX dsDNA unwinding reactions exhibit an apparent lag both in the disappearance of dsDNA and in the appearance of ssDNA may indicate that the propagation of DNA unwinding is slow, relative to the initiation of unwinding. In this case, there would be a significant accumulation of partially unwound DNA intermediates during the early time points of the reaction which would not be detected by the gel assay; ssDNA would not appear in the gel assay until the strands were completely separated. In contrast, if initiation of DNA unwinding was slow and the subsequent propagation of unwinding was fast, then every DNA molecule, in effect, either would be completely unwound or would not yet have initiated unwinding. In this case, the appearance of ssDNA in the agarose gel assay would be expected to follow a linear time course. The shorter apparent lag time observed for the unwinding of pUC18 DNA (2686 base pairs) compared to ϕX DNA (5386 base pairs) is probably due to a faster completion of unwinding of the shorter DNA.

In order to analyze our DNA unwinding data more closely for the existence of partially unwound intermediates, we constructed a calibration curve in which the ATP hydrolysis activity of helicase II (200 nM) was measured as a function of ssDNA concentration (Figure 8). We then used this calibration curve to calculate the instantaneous rates of ATP hydrolysis that would be expected in the dsDNA-dependent ATP hydrolysis reaction, as judged by the amount of ssDNA that was detected in the agarose gel assays at each time point during the DNA unwinding reactions shown in Figure 7. In Figure 9, these calculated rates of ATP hydrolysis are plotted as a function of time and are compared to the observed instantaneous rates of ATP hydrolysis that were derived from

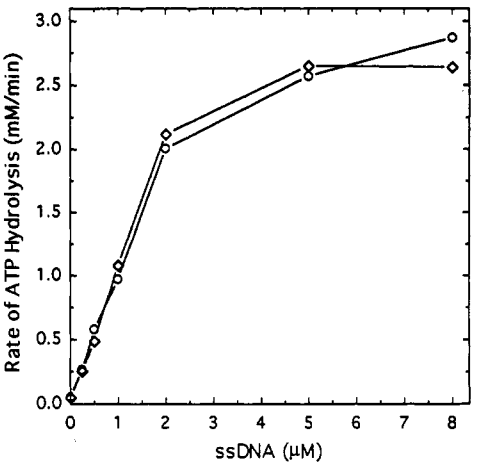

FIGURE 8: Rate of ATP hydrolysis as a function of ssDNA concentration. Reactions contained 25 mM Tris-HCl (pH 7.5), 4.5 mM $MgCl_2$, 4 mM ATP, 200 nM helicase II, and the indicated concentrations of pUC18 ssDNA (○) or ϕX ssDNA (◇). The reactions were carried out at 37 °C. The points represent the initial rates of ATP hydrolysis at each ssDNA concentration.

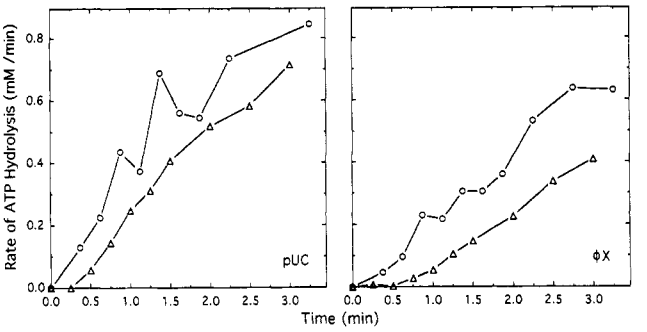

FIGURE 9: Comparison of observed and calculated rates of ATP hydrolysis during DNA helicase II-promoted DNA unwinding. Instantaneous rates of ATP hydrolysis were calculated for various time points in the pUC18 and ϕX DNA unwinding reactions; these calculations were based on the amount of ssDNA detected at these time points by the agarose gel assays shown in Figure 7 and the ssDNA-dependent ATP hydrolysis calibration curve shown in Figure 8. These calculated rates (△) are plotted as a function of time, along with the experimentally determined instantaneous rates of hydrolysis (○) which were derived from the dsDNA-dependent ATP hydrolysis time courses shown in Figure 3. See text for additional details.

the ATP hydrolysis reactions (200 nM helicase II) shown in Figure 3.

As shown in Figure 9, the experimentally observed instantaneous rates of ATP hydrolysis during the lag phase of the dsDNA-dependent ATP hydrolysis reactions are significantly higher than can be accounted for by the level of ssDNA that appears at these same time points in the agarose gel assay. The greatest difference is apparent during the first 45 s of the reactions, when the observed rate of ATP hydrolysis is as much as 4–6-fold higher than the calculated ATP hydrolysis rates for pUC18 DNA and ϕX DNA, respectively. These numbers probably represent a lower limit on the maximal degree of difference between observed and calculated ATP hydrolysis rates since the agarose gel assay fails to detect any unwound DNA during the first 0.25 min of the pUC18 reaction or the first 0.5 min of the ϕX DNA reactions. These results indicate that significant amounts of partially unwound DNA intermediates are present during the first minute of the DNA unwinding reactions which are not detected by the agarose gel assay, but which are reflected in the ATP hydrolysis activity of helicase II. This observation provides additional support for a model in which the lag phase in the dsDNA-dependent

ATPase reaction corresponds to the progressive unwinding of the dsDNA.

The results in this paper are consistent with the general model for the stoichiometric unwinding of dsDNA by helicase II shown in Figure 1. Initially, when helicase II is not bound to the dsDNA substrate, there is little ATP hydrolysis activity. The unwinding reaction probably begins with the binding of helicase II molecules to the ends of the dsDNA molecules, a step which may involve an isomerization of helicase II and the melting of this region of the DNA. As the unwinding reaction continues, additional helicase II molecules become bound to the unwound regions of the DNA molecule and become activated for ATP hydrolysis. When the DNA has been only partially unwound, however, no ssDNA will be detected by the agarose gel assay. When unwinding is complete, on the other hand, the maximal rate of ATP hydrolysis is attained, and the separated complementary single strands are detected by the gel assay. In this stoichiometric unwinding reaction, the maximal extent of DNA unwinding and the corresponding maximal (steady state) rate of ATP hydrolysis are achieved at helicase II concentrations sufficient to saturate the separated single strands. Also, if the propagation of DNA unwinding is slow relative to the rate of initiation, this model predicts that unwinding will be completed more quickly with shorter DNA molecules than with longer DNA molecules (at a fixed total nucleotide concentration of dsDNA and a saturating concentration of helicase II), consistent with the shorter dsDNA-dependent ATP hydrolysis and agarose gel DNA unwinding lag times that were obtained with pUC18 dsDNA compared to ϕX dsDNA. The greater maximal extent of unwinding that was observed for pUC18 dsDNA (85%) relative to ϕX dsDNA (70%) suggests that the capacity of helicase II to unwind a duplex DNA molecule may be limited by a competition between complete separation of the complementary single strands (and detection by the agarose gel assay) and renaturation of the partially unwound regions of the DNA molecule, and that this effect is more pronounced with longer DNAs than with shorter DNAs.

In summary, the results presented in this paper indicate that the kinetics of the dsDNA-dependent ATP hydrolysis reaction may be analyzed to monitor the progressive unwinding of duplex DNA by helicase II. The ATP hydrolysis reaction has the potential of identifying the presence of partially unwound DNA intermediates that are not detectable by standard gel electrophoresis assays. We are now carrying out additional experiments aimed at developing a more complete description of the kinetic mechanism of this reaction.

ACKNOWLEDGMENT

We gratefully acknowledge Dr. Tim Lohman and Dr. Gregory Runyon for furnishing *E. coli* strain N4830/pTL51 and for providing their detailed DNA helicase II purification procedure prior to publication.

REFERENCES

Abdel-Monem, M., Chanal, M. C., & Hoffmann-Berling, H. (1977a) *Eur. J. Biochem. 79*, 33–38.

Abdel-Monem, M., Durwald, H., & Hoffmann-Berling, H. (1977b) *Eur. J. Biochem. 79*, 39–45.

Caron, P. R., Kushner, S. R., & Grossman, L. (1985) *Proc. Natl. Acad. Sci. U.S.A. 82*, 4925–4929.

Cox, M. M., & Lehman, I. R. (1981) *Proc. Natl. Acad. Sci. U.S.A. 78*, 3433–3437.

Hickson, I. D., Arthur, H. M., Bramhill, D., & Emerson, P. T. (1983) *Mol. Gen. Genet. 190*, 265–270.

Husain, I., Van Houten, B., Thomas, D. C., Abdel-Monem, M., & Sancar, A. (1985) *Proc. Natl. Acad.* Sci. *U.S.A. 82*, 6774–6778.

Kuhn, B., Abdel-Monem, M., Krell, H., & Hoffmann-Berling, H. (1979) *J. Biol. Chem. 254*, 11343–11350.

Kumura, K., & Sekiguchi, M. (1984) *J. Biol. Chem. 259*, 1560–1565.

Lahue, R. S., Au, K. G., & Modrich, P. (1989) *Science 245*, 160–164.

Maniatis, T., Fritsch, E. F., & Sambrook, J. (1982) *Molecular Cloning: A Laboratory Manual*, Cold Spring Harbor Laboratory Press, Cold Spring Harbor, NY.

Matson, S. W., & George, J. W. (1987) *J. Biol. Chem. 262*, 2066–2076.

Matson, S. W., & Kaiser-Rogers, K. A. (1990) *Annu. Rev. Biochem. 59*, 289–329.

Runyon, G. T., & Lohman, T. M. (1989) *J. Biol. Chem. 264*, 17502–17512.

Runyon, G. T., Bear, D. G., & Lohman, T. M. (1990) *Proc. Natl. Acad. Sci. U.S.A. 87*, 6383–6387.

Runyon, G. T., Wong, I., & Lohman, T. M. (1993) *Biochemistry 32*, 602–612.

Taucher-Scholz, G., & Hoffmann-Berling, H. (1983) *Eur. J. Biochem. 137*, 573–580.

Weinstock, G. M., McEntee, K., & Lehman, I. R. (1979) *Proc. Natl. Acad. Sci. U.S.A. 76*, 126–130.

Yodh, J. G., & Bryant, F. R. (1992) Keystone Symposia on Molecular and Cellular Biochemistry, *J. Cell. Biochem., Abstr. Suppl. 16B*, p 81, Wiley–Liss, Inc., New York.